Supplemental Figure legends

Figure S1. *f*EM reconstruction of AIY, VCSC glia and epidermal cell *hyp7* in *cima-1(wy84)* mutants. Related to Figure 1 and Figure 6

(A) AIY (green) and VCSC glia (red) are simultaneously visualized in wild type animals Dashed box corresponds to the region reconstructed in (B).

(B) Reconstruction of the left AIY (green) and the VCSC glia (red) using micrographs for wild-type animals available from WormImage (www.wormimage.org). The micrographs used for the reconstruction were originally photographed to describe *C. elegans* nervous system connectivity in (White, 1986)) and were made available to us by Dr. David Hall (Albert Einstein College of Medicine). We reconstructed the Zone 1 and Zone 2 regions for both the N2U and JSH datasets. The reconstruction shown here corresponds to the N2U dataset, but similar results were observed for the JSH dataset (data not shown). Note that in wild type animals, the VCSC glia ensheath the Zone 2 region, but not the Zone 1 region, consistent with what we saw with our fluorescent and GRASP markers.

(C and D) Representative cross-section EM micrographs for the Zone 1 region in wild type animals. In (C), the image corresponds to the JSH dataset, which was obtained from a wild-type L4 animal. In (D), the image corresponds to the wild-type adult N2U dataset. In both images, AIY is pseudocolored green and highlighted with a dashed line. Note the absence of dense projections or synaptic vesicles in this region of the AIY neurite (compare to Fig. 5A, where dense projections and synaptic vesicles are seen in the AIY neurite). We inspected all wild-type Zone 1 EM micrographs for JSH and N2U animals, and did not detect dense projections or vesicles in any of them, consistent with what we observed for our synaptic markers in AIY.

(E) As in (A), but *cima-1(wy84)* mutant adult animal. Dashed box corresponds to the region reconstructed in (F).

(F) Reconstruction of AIY (green), VCSC glia (red) and epidermal cell (blue) from a *cima-1(wy84)* mutant adult animal by using fluorescent EM (*f*EM). The AIY neurite was identified by the cell-specific expression of GFP. VCSC glia and epidermis were identified by cell position.

(G and H) Representative cross-section EM micrographs for the Zone 1 region in two *cima-1(wy84)* mutant animals visualized by *f*EM. AIY is pseudocolored in green and highlighted with a dashed line. Unlike wild type animals, in *cima-1(wy84)* adult animals we observed dense projections and synaptic vesicles in the Zone 1 region. In (G) we highlight a neighboring neuron onto which the ectopic AIY dense projection could be forming.

Scale bars in G and H also apply to C and D.

Figure S2. CIMA-1 is a member of SLC17 family. Related to Figure 3

A diagram of phylogenic relationship among solute carrier transporters. Phylogenic topology was based on the cluster W alignment of SLC17 family proteins from human (Hs: *Homo sapiens*), mouse (Mm: *Mus musculus*), honeybee (Ap: *Apis mellifera*), fruit fly (Dm: *Drosophila melanogaster*), sea urchin (Sp: *Strongylocentrotus purpuratus*), sea squirt (Ci: *Ciona intestinalis*), nematode (Ce: *Caenorhabditis elegans*). Two human SLC37 family proteins and one SLC16 family protein were selected to root the tree. The tree is constructed by using the NJ (neighbor-joining) method (Saitou and Nei, 1987). The tree is made with NJ (neighbor-joining) method (Saitou and Nei, 1987). The branch lengths correspond to evolutionary distances and were computed using the Poisson correction method (Zuckerkandl and Pauling, 1965). The unit is the number of amino acid substitutions per site. Evolutionary analyses were conducted in MEGA5 (Tamura et al., 2011). As shown in the tree, *cima-1* forms a cluster with SLC17, but not with SLC16 or SLC37.SLC: solute carrier, PhosT: Phosphate transporter, Hs SLC37: sugar phosphate exchanger, Hs SLC16: monocarboxylate transporter 2.

Figure S3. *cima-1* is expressed and required in epidermal cells. Related to Figure 4
(A-H), CIMA-1(genomic)::SL2::GFP is expressed in the embryo (A, B), larval (C, D), and adult stages (E-H) in the intestine (D, as indicated by the arrow) and in epidermal cells (D, E and G, as indicated by arrow heads), but not in the AIY interneuron (E, F) or VCSC glia (G, H) (as indicated by asterisk). The AIY interneuron and the VCSC glia were co-labeled with cytoplasmic mCherry (F, H).
(I) Cell specific expression of *cima-1* cDNA in neurons/intestine (*aex*-3 promoter) and in VCSC glia (*hlh-17* promoter) does not result in rescue. However, endogenous expression (*cima-1* promoter) or tissue-specific expression in epidermal cells (*rol-6*, *dpy-7* and *col-19* promoter) rescues the AIY presynaptic defect. P*col-19* promoter drives expression after larval stages and in epidermal cells (Cox and Hirsh, 1985; Liu and Ambros, 1991). Therefore rescue using the P*col-19* suggests that *cima-1* acts post-developmentally in epidermal cells. Error bars are s.e.m..
(J-Y) CIMA-1 protein fused to RFP (CIMA-1::RFP) is coexpressed in epidermal cells with mitochondrial marker TOM20::YFP (J-M), early endosomal marker GFP::RAB-5 (N-Q), later endosome GFP::RAB-7 (R-U), and lysosomal marker GFP::CUP-5 (V-Y). White arrows indicate CIMA-1::RFP, arrow heads indicate GFP-marked proteins and orange arrows indicate the colocalization of CIMA-1::RFP and GFP-marked proteins.. Notice that CIMA-1::RFP is largely colocalized with lysosomal marker GFP::CUP-5. Consistent with this, Pearson's correlation coefficient for CIMA-1 and CUP-5 is 0.53 (for the other markers: CIMA-1 and TOM20 is 0.021; CIMA-1 and RAB-5 is 0.22; CIMA-1 and RAB-7 is 0.28). The scale bar in J applies to N, R, and V; scale bar in K applies to L-M, O-Q, S-U and W-Y.

Figure S4. Morphological phenotypes in *cima-1(wy84)* adult animals. Related to Figure 4
(A) Quantification of length, width, pharyngeal morphology and length of AIY Zone 1 (as indicated in Figure 1A) for wild type and *cima-1(wy84)* animals (L4 and adults, as stated in the table). Parameters are indicated in the schematic. Note that *cima-1(wy84)* mutant animals are slightly longer for both body and AIY Zone 1 length, although the pharyngeal morphology is similar to wild type animals. The numbers are mean±s.d.
(B and C) *cima-1(wy84)* animals 12 hours after L4 (B) and *cima-1(wy84)* animals two days after L4. (C) Some 2-3 day-old *cima-1(wy84)* mutants burst at the vulva. All of the analyses presented here regarding glia positions and presynaptic pattern in AIY were done in *cima-1(wy84)* adult animals before this period.
(D-G) Wild type (D and E) and *cima-1(wy84)* (F and G) adult animals labeled with epidermal cell junction marker AJM-1::GFP. No differences were noticed in the localization of AJM-1::GFP or regarding cellular fusions during development.
(H-K) Wild type (H and I) and *cima-1(wy84)* (J and K) adult animals labeled with epidermal GFP (*cima-1* promoter) and AIY mCherry (*ttx-3* promoter) were imaged and characterized (n>10 animals). No abnormalities were noticed regarding epidermal cells morphology between *cima-1(wy84)* and wild type animals.
(L -O) p*rab-3*::GFP and p*hlh-17::*mCherry in wild type (L and M) and *cima-1(wy84)* mutant (N and O). No abnormalities were noticed regarding neuronal distribution between *cima-1(wy84)* and wild type animals, but notice how glia are posteriorly distended in *cima-1(wy84)* mutant adults.

Figure S5. Expressivity of the AIY presynaptic defect in *cima-1(wy84)* is affected by size of the animal. Related to Figure 4
(A-C) Morphology of wild type, *dpy-4(e1166)* and *lon-3(e2175)* animals.
(D-I) AIY presynaptic marker GFP::RAB-3 in wild type (D), *cima-1(wy84)* (G), *cima-1(wy84) dpy-4(e1166)* (E), *cima-1(wy84) dpy-7(e88)* (H), *lon-3(e2175)* (F) and *cima-1(wy84) lon-3(e2175)* (I)

animals. Note that *dpy* mutants suppress *cima-1(wy84)* AIY presynaptic defect, and *lon-3(e2175)* enhances *cima-1(wy84)* phenotype.
(J-K) Quantification of AIY presynaptic pattern (J) and Zone 1 length (K). In (J), the ratio of the presynaptic length (see Figure 1K) is a metric that reflects the presynaptic pattern of AIY. Note how AIY presynaptic ratio defect in *cima-1(wy84)* animals is suppressed by *dpy-4(e1166)* and *dpy-7(e88)* and enhanced by *lon-3(e2175)*. In (K), for wild type and *cima-1(wy84)* animals, the length of AIY Zone 1 was measured at larval L1, L4 and adult stages. For *lon-3(e2175)* and *cima-1(wy84) dpy-4(e1166)* animals, it was measured only at adult stage. Note that at L1 or L4 stage, the length of AIY Zone 1 is not significantly different between wild type and *cima-1(wy84)* mutant animals. At adult stage, however, it is significantly longer in *cima-1(wy84)* animals. Although AIY Zone 1 is longer in *lon-3(e2175)* mutants (see K), *lon-1(e2175)* animals do not phenocopy *cima-1(wy84)* mutants. Therefore, it is not the increase in the length of the AIY axon that causes ectopic synapses in *cima-1(wy84)* mutants, rather it is a specific requirement for *cima-1.* Error bars are s.e.m. **: $p<0.01$, ***: $p<0.001$ by t-test comparison.

Figure S6. Longitudinal analyses of glial morphology, RIA position and AIY presynaptic pattern in wild type and *cima-1(wy84)* animals. Related to Figure 5
(A-H) A single wild type animal labeled with AIY presynaptic CFP::RAB-3(pseudocolored green), RIA postsynaptic GLR-1::YFP (pseudocolored blue) and VCSC glia cytoplasmic mCherry was imaged at juvenile L4 stage (A-D), and 48 hours later at adult stage (E-H).
(I-P) A single *cima-1(wy84)* animal was imaged at juvenile L4 (I-L) and 48 hours later at adult stage (M-P). Arrows highlight the end of Zone 2 and beginning of Zone 1, and brackets corresponds to ectopic presynaptic sites in Zone 1 region.

Figure S7. *egl-15(n484), but not unc-40(e271),* suppress *cima-1*. Related to Figure 7
(A-C) Presynaptic marker GFP::RAB-3 in wild type (A) or *unc-40(e271)* mutants (B). Schematic drawing of a wild type animal in (C).
(D-F) As in (A-C), but in *cima-1(wy84*) adult animals (D) or *cima-1(wy84) unc-40(e271)* double mutants adult animals (E).
(G) Quantification of the percentage of animals displaying ectopic presynaptic sites in the Zone 1 region of AIY. Note how *unc-40(e271)* does not suppress the number of animals displaying ectopic presynaptic sites in Zone 1 in *cima-1(wy84)*. Error bars represent 95% confidential interval. n.s.: not significant based on Fisher's exact test.
(H) Quantification of intensity of AIY synaptic vesicle marker GFP::RAB-3 in larval stage 1 (L1) animals for indicated genotypes. AU: arbitrary unit.
(I) Quantification of the percentage of animals displaying ectopic presynaptic sites in Zone 1 for examined genotypes. Error bars represent 95% confidential interval. n.s.: not significant, ** $p<0.01$, *** : $p<0.001$ between groups by using Fisher's exact test.

Extended Experimental Procedures

Strains

Worms were raised on NGM plates at 22°C using OP50 *E. coli* as a food source (Brenner, 1974). Strains used in this study were listed in table S1.

cima-1(wy84) cloning

Fosmids injected for cloning *cima-1(wy84)* includes: WRM068bB06, WRM0617aA03, WRM0633dE08, WRM0630bH07, WRM0618aA07, WRM067bC05, WRM0612aH07, WRM068aE11, WRM0616bG10, WRM066dA02, WRM0623cD10, WRM0612BA03, WRM0615cC03, WRM0620cA08, WRM067aG11, WRM065aD01, WRM068dD06, WRM0623cC07.

Protein blot

40-60 synchronized L4 animals were collected and boiled in 10µl M9 and 10µl 2x sample buffer (from Bio-Rad Life Science) for 10 minutes before loading to 4-15% gradient polyacrylamide gels (from Bio-Rad Life Science). Blots were probed with monoclonal antibodies recognizing the following epitopes: GFP (HRP conjugated antibody from Cell Signaling at 1:500 dilution); HA (HRP conjugated antibody from Cell Signaling Technology clone 6E2 at 1:500 dilution); actin (HRP conjugated antibody from Santa Cruz Biotechnology at 1:10000 dilution), or polyclonal anti-EGL-15 Crackle (a gift from M. Stern used at 1:1000 dilution). The secondary antibody (HRP conjugated goat anti-rabbit antibody from Cell Signaling Technology) was diluted 1:2000.

We used EGL-15 Crackle antibody (a gift from M Stern), which recognizes both isoform 5A and 5B expressed in all tissues (Lo et al., 2008). We observed that we could detect a 141kDa protein band in wild type animals (Figure 7G), but not in *egl-15(n1477)* or *egl-15(n1457)* mutants. *egl-15(n1477)* and *egl-15(n1457)* carry early stop at W878 and Q896, which produce the C-terminus truncated EGL-15 that was not recognized by the antibody (Figure 7G, data not shown). These findings, which are consistent with unpublished protein characterizations, suggest that EGL-15 runs as a 141kDa protein band (M Stern, personal communication). Then we examined the protein levels of the EGL-15(5A) specific isoform in epidermal cells. To achieve this, we generated transgenic animals expressing C-terminus HA- tagged EGL-15(5A) just in epidermal cells, and probed protein levels by western blots in both *cima-1(wy84)* and wild type animals.

Quantification and statistics

For the AIY presynaptic pattern analyses, animals were synchronized at L1, L4 and adult stages. We calculated the ratio of the presynaptic region in a three-step process: First, we measured the length of the presynaptic region in the ventral part of the AIY neurite (Zone 2 in wild-type animals, Zone 2 and presynaptic Zone 1 in *cima-1* mutants). Second, we measured the length of Zone 3. Finally, we divided first measurement by total (measurement 1+2). The quantifications for the rescue experiments were done using a compound microscope (model DM5000 B; Leica). For each construct, multiple transgenic lines were generated and quantified. For quantifications of *cima-1(wy84)* suppression, animals were imaged using a confocal microscope. The AIY presynaptic pattern was scored as wild type in confocal micrographs in which the AIY Zone 2 presynaptic sites were located proximal to the RIA postsynaptic sites. In strains in which RIA was not imaged, we scored the Zone 2 position as wild type if it was located anterior to the pharyngeal grinder, or if its length was 11 µm or shorter. VCSC glia

ablation was performed by expressing caspase fragments cell-specifically in cephalic sheath glia using the *hlh-17* promoter (Chelur and Chalfie, 2007; McMiller and Johnson, 2005; Yoshimura et al., 2008). An integrated cephalic sheath glial cytoplasmic GFP marker (Yoshimura et al., 2008) was used in the caspase transgenic lines to determine if VCSC glia were successfully ablated. Protein blot was quantified with Image Lab 4.1 (Bio-Rad). For each experiment, EGL-15::HA was normalized using actin intensity. The fold-increase in *cima-1* mutant animals was established using wild-type as a baseline.

Statistical analyses regarding the presynaptic pattern distribution, tissue specific and fosmid rescue, AIY Zone 1 length analyses, presynaptic puncta, intensity quantification, and protein levels were achieved using Student's T test. All other statistical analyses were done using Fisher's exact test.

Constructs

pTB84 [p*dpy-7::egl-15(5A)*], pTB99 [*pdpy-7::egl-15(5A)ecto*], and pTB114 [pF25B3.3:: *egl-15(5A)*] were kindly provided by Dr. H. Bülow. NH112 (*EGL-15)* were kindly provided by T. Kinnunen. P*dpy-4::gfp::cup-5* was built modified from pHD423, which was kindly provided by Dr. H. Fares. P*dpy-4::tom20::yfp*, P*dpy-4::gfp::rab-7*, P*dpy-4::gfp::rab-5* were modified from P*mig-13::tom20::yfp*, P*mig-13::gfp::rab-7*, P*mig-13::gfp::rab-5* from Dr. K. Shen. The remaining constructs were listed in table S2.

Reference

Brenner, S. (1974). The genetics of Caenorhabditis elegans. Genetics *77*, 71-94.

Chelur, D.S., and Chalfie, M. (2007). Targeted cell killing by reconstituted caspases. Proc Natl Acad Sci U S A *104*, 2283-2288.

Cox, G.N., and Hirsh, D. (1985). Stage-specific patterns of collagen gene expression during development of Caenorhabditis elegans. Mol Cell Biol *5*, 363-372.

Liu, Z., and Ambros, V. (1991). alternative temperal control systems for hypodermal cell differentiation in *Carnorhabditis elegans*. Nature *350*, 162-165.

Lo, T.W., Branda, C.S., Huang, P., Sasson, I.E., Goodman, S.J., and Stern, M.J. (2008). Different isoforms of the C. elegans FGF receptor are required for attraction and repulsion of the migrating sex myoblasts. Dev Biol *318*, 268-275.

McMiller, T.L., and Johnson, C.M. (2005). Molecular characterization of HLH-17, a C. elegans bHLH protein required for normal larval development. Gene *356*, 1-10.

Saitou, N., and Nei, M. (1987). The neighbor-joining method: a new method for reconstructing phylogenetic trees. Mol Biol Evol *4*, 406-425.

Tamura, K., Peterson, D., Peterson, N., Stecher, G., Nei, M., and Kumar, S. (2011). MEGA5: molecular evolutionary genetics analysis using maximum likelihood, evolutionary distance, and maximum parsimony methods. Mol Biol Evol *28*, 2731-2739.

White, J.G., E. Southgate, J. N. Thomson, S. Brenner (1986). The Structure of the Nervous System of the Nematode Caenorhabditis elegans. Philosophical Transactions of the Royal Society of London Series B, Biological Sciences, *314*, 1-340.

Yoshimura, S., Murray, J.I., Lu, Y., Waterston, R.H., and Shaham, S. (2008). mls-2 and vab-3 Control glia development, hlh-17/Olig expression and glia-dependent neurite extension in C. elegans. Development *135*, 2263-2275.

Zuckerkandl, E., and Pauling, L. (1965). Evolutionary divergence and convergence in proteins. In Evolving Genes and Proteins, V.B.a.H.J. Vogel, ed. (New York.: Academic Press), pp. pp. 97-166.

Supplemental Figure 1

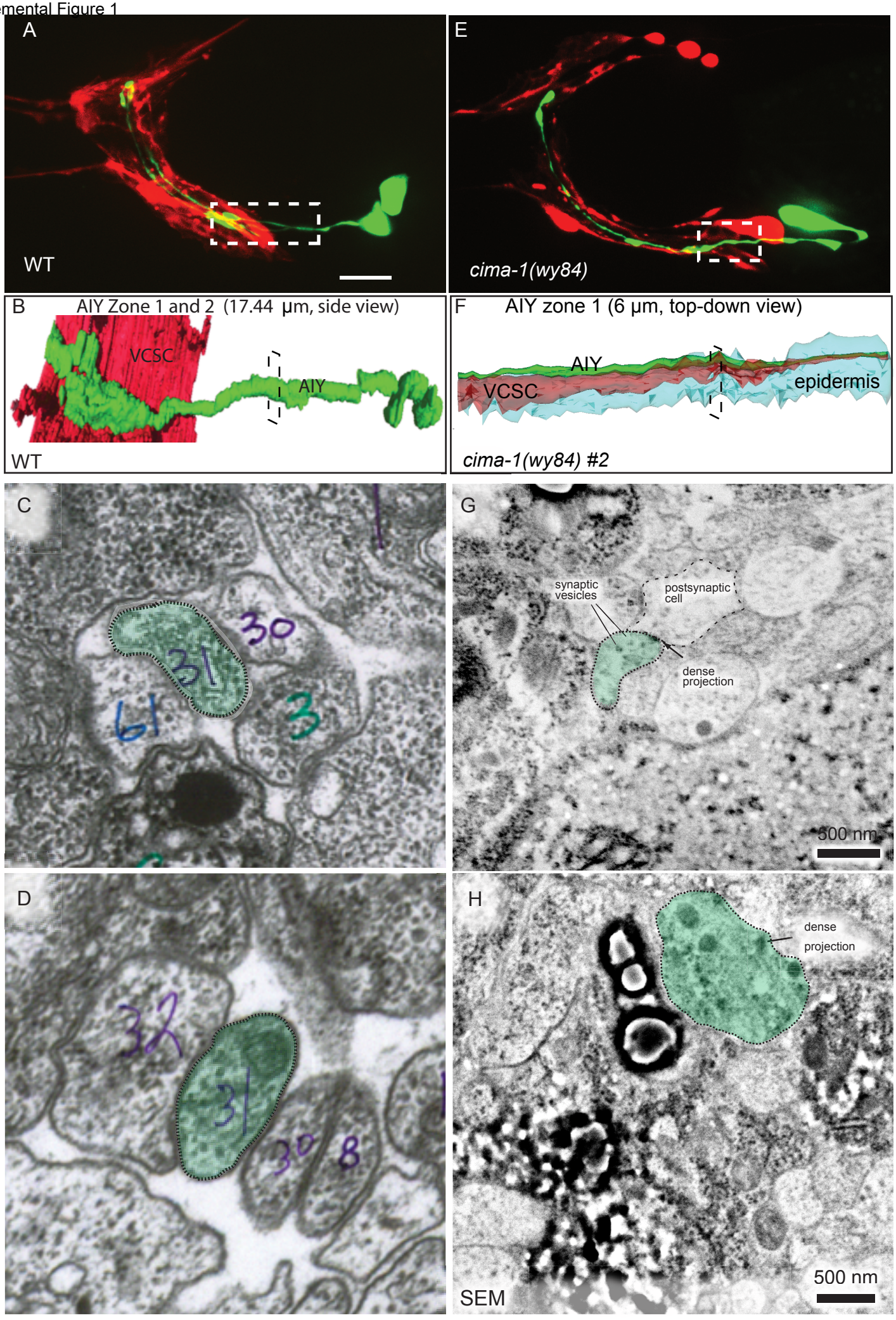

Supplemental Figure 2

Figure 32

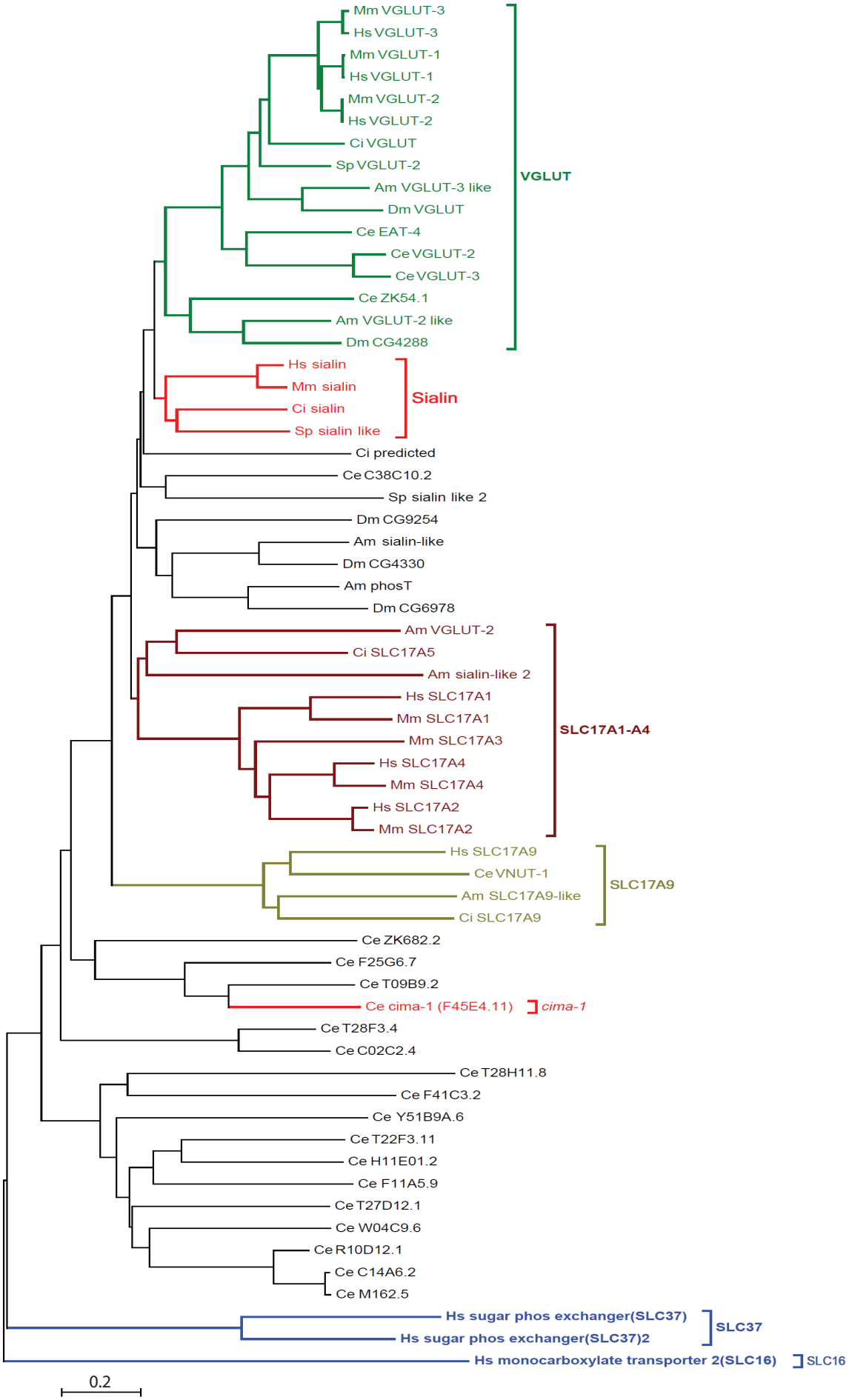

Supplemental Figure

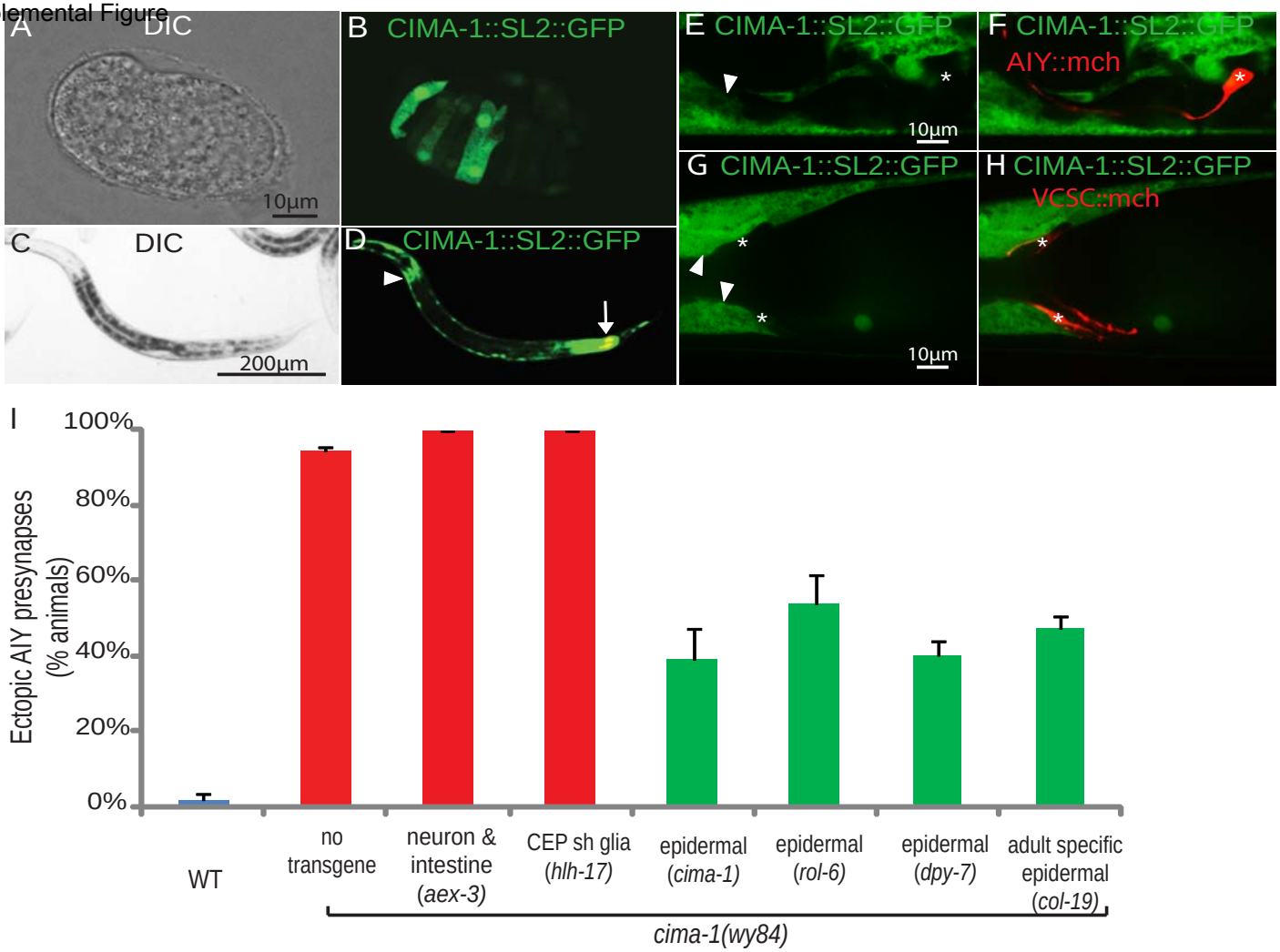

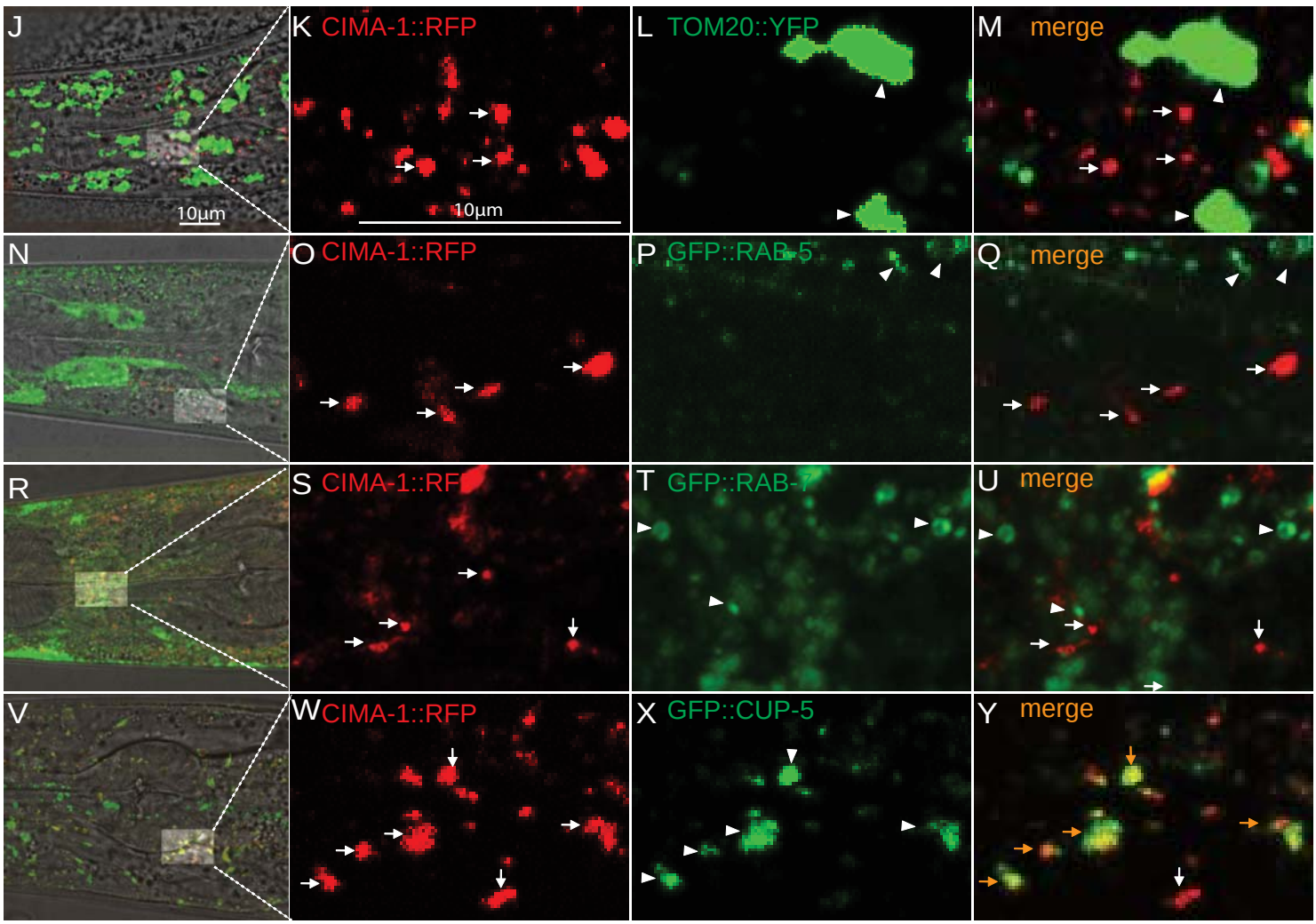

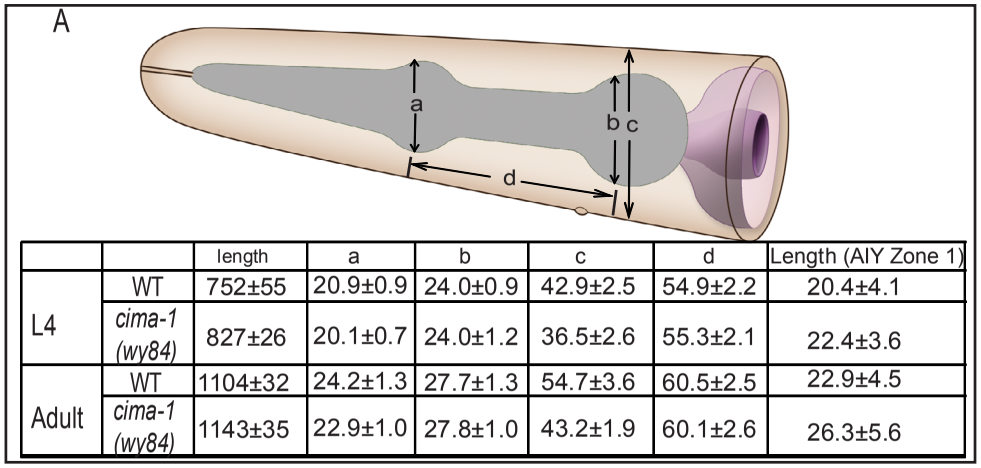

		length	a	b	c	d	Length (AIY Zone 1)
L4	WT	752±55	20.9±0.9	24.0±0.9	42.9±2.5	54.9±2.2	20.4±4.1
	cima-1 (wy84)	827±26	20.1±0.7	24.0±1.2	36.5±2.6	55.3±2.1	22.4±3.6
Adult	WT	1104±32	24.2±1.3	27.7±1.3	54.7±3.6	60.5±2.5	22.9±4.5
	cima-1 (wy84)	1143±35	22.9±1.0	27.8±1.0	43.2±1.9	60.1±2.6	26.3±5.6

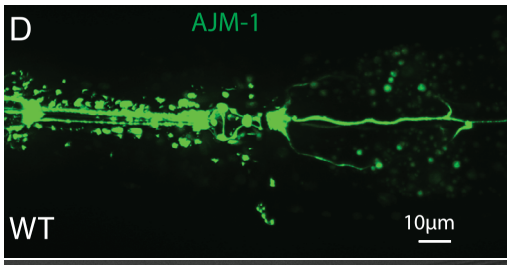

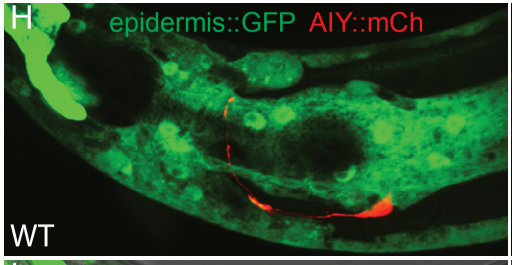

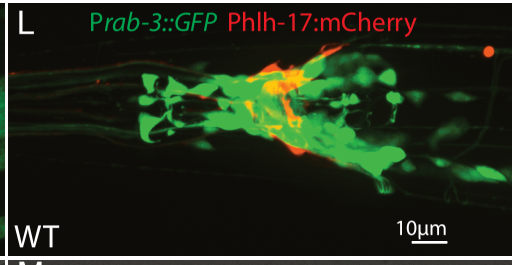

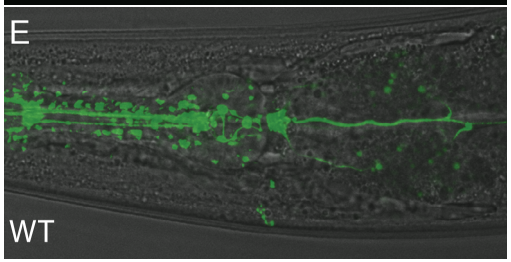

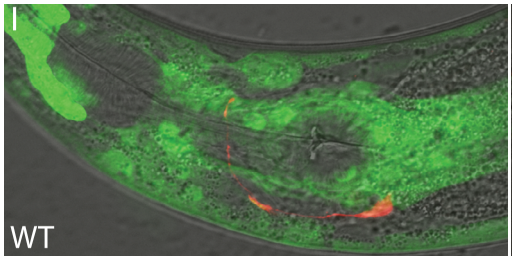

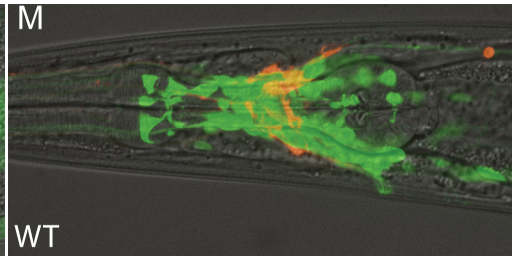

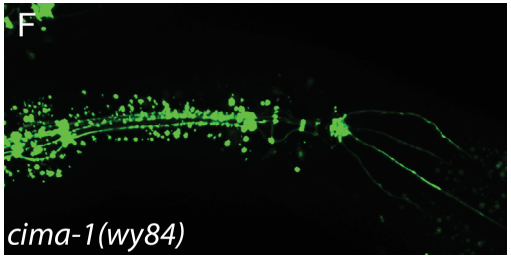

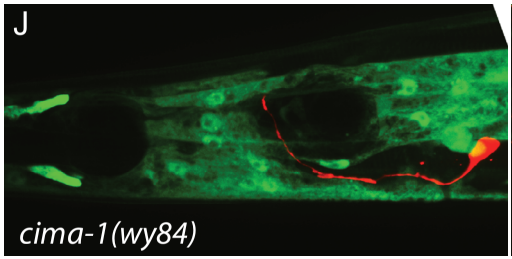

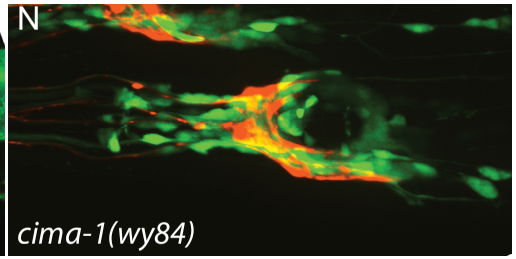

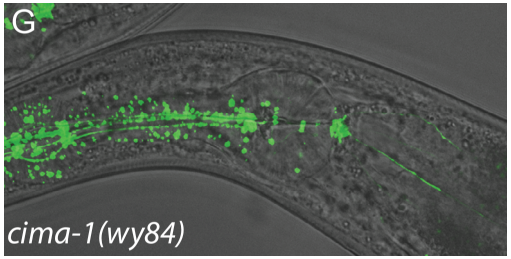

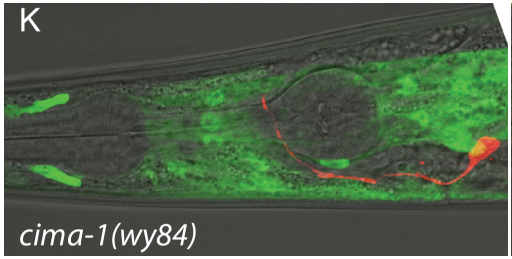

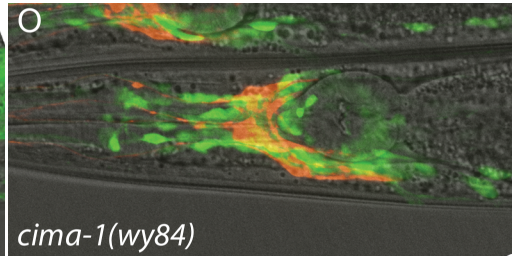

Supplemental Figure 5

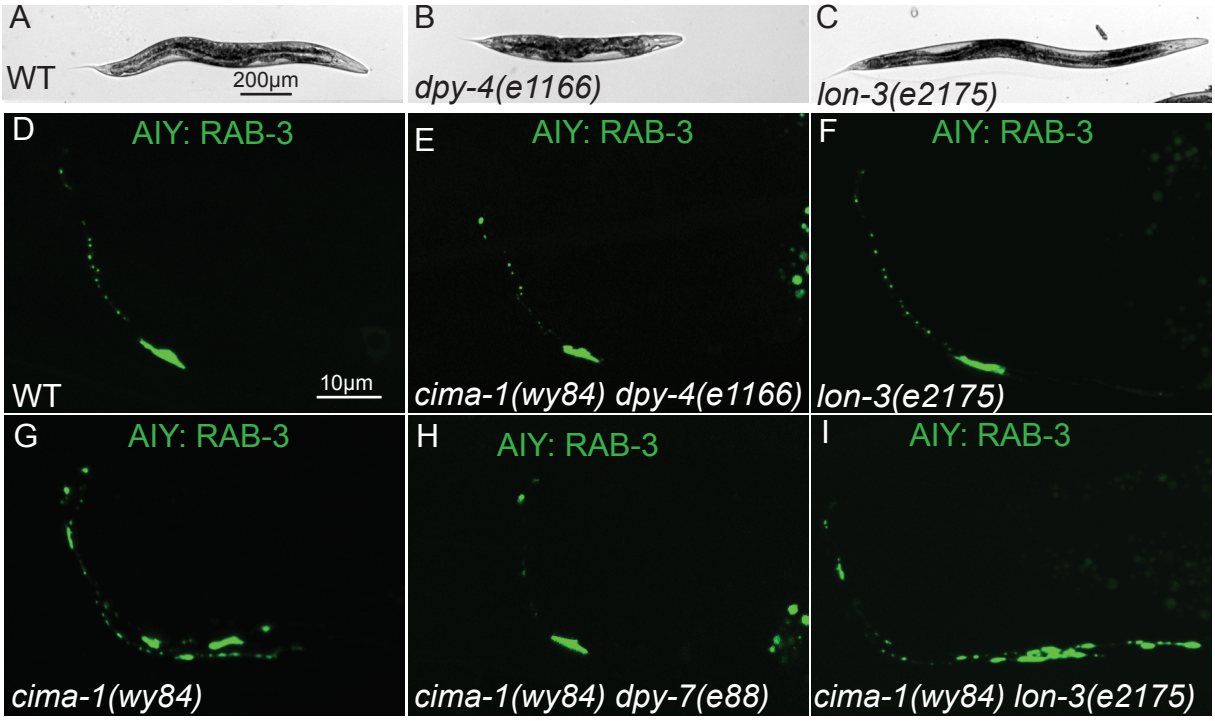

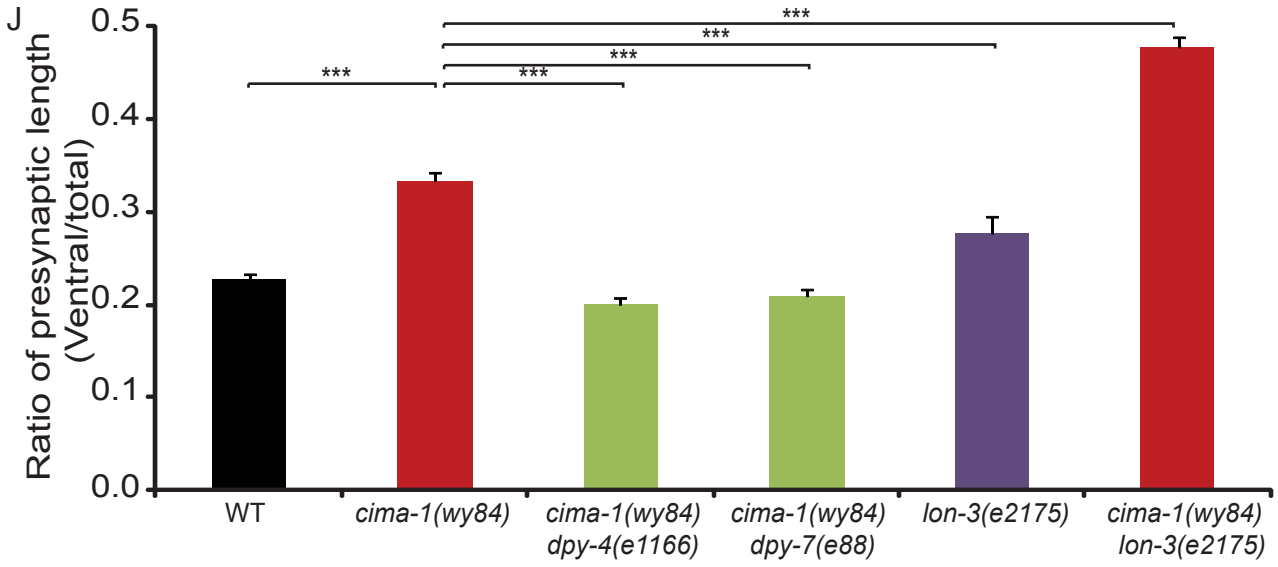

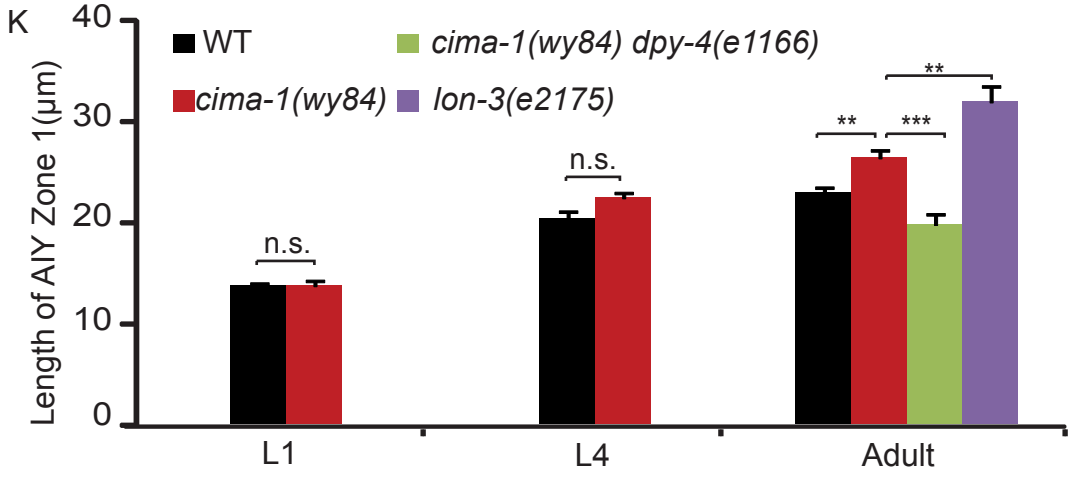

Supplemental Figure 6

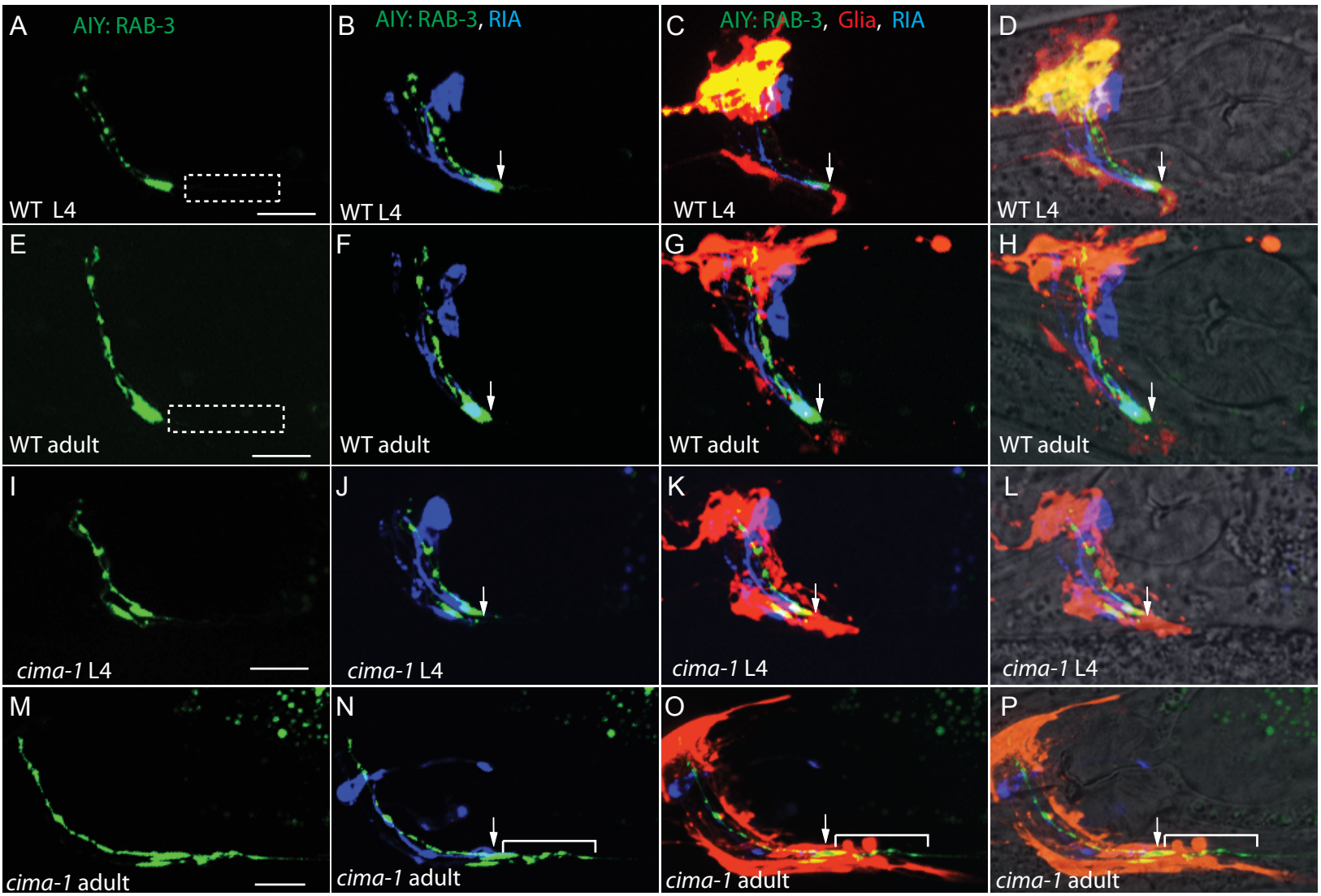

Supplemental Figure 7